Design Trades for Environmentally Friendly Broadband LEO Satellite Systems

Mark A. Sturza
3C Systems Company

Gemma Saura Carretero
Viasat, Inc.

ABSTRACT

Humanity faces an existential crisis; space debris are at risk of becoming the equivalent of a "drifting island of plastic." Large constellation (LC) systems plan to operate tens of thousands, or even hundreds of thousands, of satellites in low Earth orbit (LEO), posing the threat of an inglorious end to the Space Age. Satellites that cannot maneuver, cannot avoid collisions. Even satellites that can maneuver, can be involved in collisions. Collisions between LEO satellites tend to be catastrophic resulting in large numbers of new debris objects spread across LEO altitudes.

A model is developed to explore the dependence of the time to Kessler Syndrome on the number of satellites, the satellite sizes, and the orbits of LCs. Simulations show: 1) that LCs of small satellites (<25 kg) are significantly safer than constellations of medium (25 to 300 kg) or large (>300 kg) satellites, and 2) that if LCs of medium or large satellite are deployed, they are safer at lower orbits, such as 450-km rather than at 600-km or 1,200-km orbits. The orbital capacity (number and type of satellites that can be sustainably deployed) and tipping point (at which it is no longer possible to avoid a Kessler Syndrome by ceasing launches) concepts are demonstrated.

1. INTRODUCTION

Humanity faces an existential crisis; space debris are at risk of becoming the equivalent of a "drifting island of plastic" [1]. Large constellation (LC) systems plan to operate tens of thousands, or even hundreds of thousands, of satellites in low Earth orbit (LEO) [2], posing the threat of an inglorious end to the Space Age. A "take risks and fail often" approach to new technology is being extended to space without considering that mistakes in space cannot be cleaned up as easily as they can on Earth.

Satellites that cannot maneuver, cannot avoid collisions. Loss of maneuverability can result from failures of satellite sub-systems in the maneuver chain or from collisions with small (untracked) objects that disable these subsystems. Passive deorbit times can be minimized with lower LEO altitudes and larger area-to-mass ratios but can still require years depending on the solar cycle and larger area-to-mass ratios realized by increasing area can lead to increased collision risk.

Even satellites that can maneuver, can be involved in collisions. Conjunction warnings may not be generated, not all lethal debris are trackable. Every time a satellite is not maneuvered in response to a low probability conjunction warning, there is a non-zero collision risk that depends on the space situational awareness (SSA) accuracy. Additionally, every time a satellite is maneuvered, there is another non-zero probability that the maneuver will result in a collision. In both cases, with a sufficient number of conjunctions occurring, even six sigma events can become likely.

Collisions between LEO satellites are typically catastrophic resulting in large numbers of new debris objects spread across LEO altitudes. For example, there are currently 1439 tracked debris objects in orbit from the 2009 collision between Iridium-33 and COSMOS-2251 [3]. Even though the collision occurred at 800-km, the debris' apogees now range from 400 km to over 1,600 km.

Constellations are appropriately analyzed over their orbital lifecycles. LCs are incrementally deployed, and satellites are replenished as they fail, reach end-of-life, or are replaced with more capable models. This replenishment can be reasonably modeled to continue until the constellation is no longer economically viable. The result is a continuing process of orbit raising and phasing, and a combination of active and passive deorbiting.

Sub-system failures and small object collisions can be mitigated with sub-system redundancy, and small objects collision can be further mitigated with shielding. Operational techniques, such as initiating deorbit immediately after the (N – 1)-th failure with N-th redundancy, can be used to improve the effective satellite reliability.

The debris environment naturally evolves over time as objects decay and new objects are created by collisions between existing debris objects. Satellite collisions can cause step increases in the debris population. In addition, there are over 900 derelict rocket bodies remaining in orbit which pose further debris generating risk.

Previous work [4] using a simplistic model showed that reducing the number of non-maneuverable satellites significantly increases the time to Kessler Syndrome, a self-sustaining collision cascade [5]. Another approach [2] used simplified rate equations to model population evolution. One of the simplifications was ignoring collisions of debris with other debris, precluding the possibility of a Kessler Syndrome.

This paper expands on the previous work with more sophisticated Markov models and Monte Carlo simulations to explore the dependence of time to Kessler Syndrome on key parameters of LCs (the number of satellites, the satellite sizes, and the orbits). The approach is not only useful in the design of environmentally friendly broadband LEO systems, but also in assessing the environmental impact of existing and planned LC systems. Further, it can help in understanding the implications of multiple LCs occupying interleaving or overlapping orbits.

While it is generally agreed that LEO is a finite resource and that collisions may lead to loss of access to space [6][7][8][9], this work can be used to help address the key questions:

1) How many satellites are too many? What is the "orbital capacity", the number and type of satellites that can be sustainably deployed in each orbit without risking a Kessler Syndrome?
2) How close are we to a "tipping point", i.e., how urgent is this issue? A tipping point in that point in time at which it is no longer possible to avoid a Kessler Syndrome by ceasing launches.

This is an active area of research with numerous contributions, including [10][11][12].

The models are described in Section 2, Section 3 discusses the simulation results, and the conclusions are summarized in Section 4.

2. MODELS

A model is developed to explore the dependence of time to Kessler Syndrome on the constellation sizes and orbits, and on the size of the satellites deployed. The key simplifying assumptions employed to create this model are:

1. Only the LCs being studied are replenished over time, other constellations and individual satellites are not replaced as they deorbit, fail, or fragment.
2. No new rocket bodies are left in orbit.
3. Collisions with debris between 1 cm and 10 cm never result in fragmentation, only the possibility of damage resulting in loss of maneuverability, and the estimated 128 million debris from 1 mm to 1 cm [13] are ignored.
4. All orbits are circular, including those of satellites, debris, and rocket bodies, and orbits are fully characterized by their altitude and inclination.
5. Objects are grouped into classes with one set of characteristics modeled for each class.
6. The probability of non-maneuverable satellites experiencing catastrophic collisions is approximated as described in Section 2.4.1.

The first three assumptions are believed to be optimistic. Further work is required to access the impact of the last three.

Objects are divided into 10 classes. At the top level, objects are categorized as satellite (S), debris (D), or rocket body (RB). Satellites are sub-categorized as maneuverable (SM) or non-maneuverable (SN). They are further sub-categorized by mass: large (SML and SNL) for mass greater than 300 kg, medium (SMM and SNM) for mass

between 25 kg and 300 kg, and small (SMS and SNS) for mass less than 25 kg. Debris are sub-categorized by diameter, large (DL) for 1 to 3 m diameter, medium (DM) for 0.3 to 1 m diameter, and small (DS) for 0.1 to 0.3 m diameter. Rocket bodies (RB) are not further sub-categorized.

For each class, the number of objects in each orbit is stored in a matrix with the structure shown in Fig. 1. The possible orbits include all altitudes between 200 km and 2,000 km in 25 km bins (δh = 25 km), and all inclinations between 0° and 180° in 10° bins (δi = 10°). The number of objects in each bin at time t_m is $X_m^{j,k}$. These matrices are initialized using Space-Track SATCAT data [3]. A total of 16,621 LEO orbits were used – 3,773 maneuverable satellites, 920 non-maneuverable satellites, 10,992 debris, and 957 rocket bodies.

Altitude (km) \ Inclination (°)		i_1	$i_2 = i_1 + \delta i$		$i_{Ni} = i_{Ni-1} + \delta i$
	$h_{Nh} = h_{Nh-1} + \delta h$	$X_m^{Nh,1}$	$X_m^{Nh,2}$		$X_m^{Nh,Ni}$
				$X_m^{j,k}$	
	$h_2 = h_1 + \delta h$	$X_m^{2,1}$	$X_m^{2,2}$		$X_m^{2,Ni}$
	h_1	$X_m^{1,1}$	$X_m^{1,2}$		$X_k^{1,Ni}$

Fig. 1. Object Flux Matrix

The LC orbit models are discussed in Section 2.1 and the object models in Section 2.2. Section 2.3 introduces the state evolution model, and the state transition probabilities are derived in Section 2.4. The object life process models are discussed in Section 2.5.

2.1 Large Constellation (LC) Orbit Models

Three LC orbits are considered: 1) 450 km altitude at 40° inclination, 2) 600 km altitude at 50° inclination, and 3) 1,200 km altitude at 60° inclination. These were selected to be representative of the LC orbits proposed for various NGSO systems [2].

2.2 Object Models

The key parameters for each object class are shown in Tab. 1. They are representative of objects in each class and are not based on any specific objects. The area-to-mass ratios (A/M) of the non-maneuverable satellites are modeled as one-half of those for the maneuverable satellites to account for tumbling.

Tab. 1. Object Class Parameters

	SML	**SMM**	**SMS**	**SNL**	**SNM**	**SNS**	**DL**	**DM**	**DS**	**RB**
Maneuverable	Yes	Yes	Yes	No	No	No	No	No	No	No
Size	L	M	S	L	M	S	L	M	S	N/A
Length (m)	10	5	1	10	5	1	2	0.6	0.2	10
Mass (kg)	500	250	15	500	250	15	100	10	1	2000
A/M (m^2/kg)	0.080	0.080	0.067	0.040	0.040	0.033	0.040	0.040	0.040	0.025
C_D	2	2	2	2	2	2	2.4	2.4	2.4	2.4

2.3 State Evolution Model

State evolution is modeled as shown in Fig. 2. Newly launched satellites start in the Maneuverable State. At each time step, there are four possibilities for evolution of maneuverable satellites (SML, SMM, SMS): 1) transition to

the Non-Maneuverable State due to a failure or due to small object collision damage that disables maneuverability, 2) transition to the Fragmentation Process as the result of a large object collision, 3) transition to the Decay Process due to atmospheric drag, or 4) remain in the Maneuverable State.

Non-maneuverable Satellites (SNL, SNM, SNS), Debris (DL, DM, DS), and Rocket Bodies (RB) are always in the Non-Maneuverable State. There are three possibilities for these objects: 1) transition to the Fragmentation Process as the result of a large object collision, 2) transition to the Decay Process due to atmospheric drag, or 3) remain in the Non-Maneuverable State.

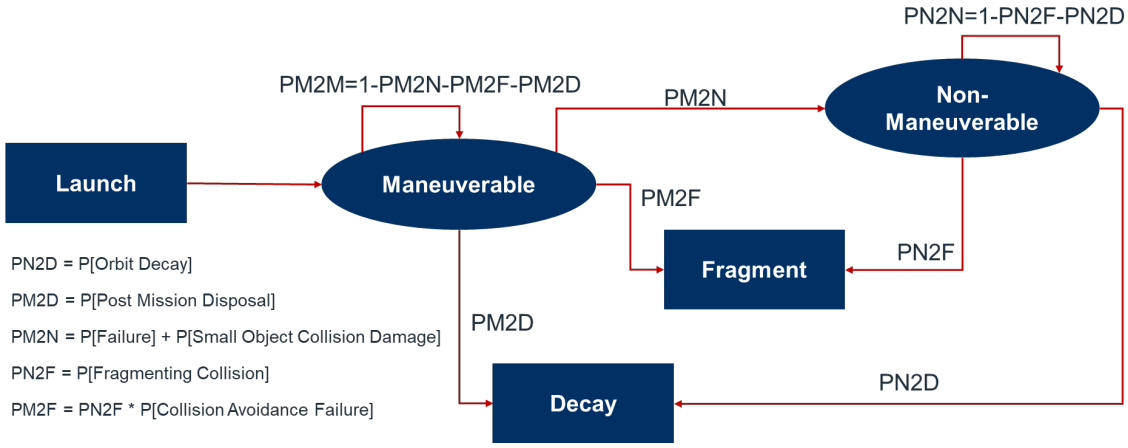

Fig. 2. State Evolution Model

2.4 Transition Probability Models

These models are used to calculate the transition probabilities for the objects in each state at each time step.

2.4.1 Probability of Non-Maneuverable Object Catastrophic Collision

PN2F is the probability of an object transitioning from the Non-Maneuverable state to the Fragmentation process. The probability that an object with radius r, in an orbit with altitude h_j, inclination i_k, and shell thickness δh experiences a collision over one orbit period at time t_m is given by

$$P_C[h_j, i_k, r, \delta h] = 1 - \prod_{q=1}^{Ni} \left(1 - P_{Ci}[h_j, i_k, r, \delta h | h_j, i_q]\right)^{X_m^{j,q}}$$

where $X_m^{j,q}$ is the total number of objects at altitude h_j and inclination i_q at time t_m, and noting that orbits are modeled as circular and the object radius, r, is much less than δh so that

$$P_{Ci}[h_j, i_k, r, \delta h | h_s, i_q] = 0 \text{ for } j \neq s$$

The probability that an object in an orbit with altitude h_j and inclination i_k experiences a collision with an object in an orbit with altitude h_j and inclination i_q is approximated by

$$P_{Ci}[h_j, i_k, r, \delta h | h_j, i_q] = \begin{cases} \left(\frac{2r}{\pi(R_e + h_j)}\right)\left(\frac{2r}{\delta h}\right) & i_k = i_q \text{ or } i_k = \pi - i_q \\ \left(\frac{2r}{\pi(R_e + h_j)}\right)^2 \left(\frac{2r}{\delta h}\right) & otherwise \end{cases}$$

The first factor in the "otherwise" value approximates the probability that both objects are inside a square with sides 2r on the surface of a sphere. When the difference in inclinations is such that the crossing angles for planes in a LC

are near 0 or π, the geometry degenerates to a single dimension, and the appropriate probability to consider is that of both objects being in a segment of the orbit circle with length 2r. The second factor is the probability that two objects in a square on the surface of the sphere are in the same cube within an orbit shell of height δh, or equivalently for the degenerative case.

2.4.2 Probability of Maneuverable Object Catastrophic Collision

The probability of a maneuverable satellite transitioning to the fragment process (PM2F) is the probability of a collision avoidance failure, either due to an untracked object, a low probability conjunction prediction being ignored, or an avoidance maneuver causing a collision. It is modeled as

$$PM2F = AvoidanceFailureRate \times PN2F$$

The avoidance failure rate is set to 0.1%, which assumes that 999 out of every 1,000 collisions that would be experienced if the satellite did not maneuver are avoided using maneuverability.

2.4.3 Probability of Maneuverable Object Orbit Decay

PM2D is the probability of a satellite object transitioning from the Maneuverable state to the Decay process. It is modeled based on the estimated satellite lifetime as

$$PM2D = \frac{\delta t}{31{,}557{,}600 \times SateliteLifetime}$$

where δt is the simulation step size in seconds and SatelliteLifetime is in years.

Satellite design life is modeled as 5 years.

2.4.4 Probability of Non-Maneuverable Object Orbit Decay

PN2D is the probability of a non-maneuverable object transitioning from the Non-Maneuverable state to the Decay process. Assuming that atmospheric drag is the only nonconservative force and modeling the orbits as circular the change in altitude over one period is given by [14]

$$\Delta h = 2\pi \left(1 - \frac{2\Omega_E \cos i}{n}\right) C_D \frac{A}{m} a^2 \rho$$

where

Ω_E is the Earth's rotation rate (rad/s)
i is the orbit inclination (rad)
n is the mean motion (rad/s)
C_D is the drag coefficient
$\frac{A}{m}$ is the area-to-mass ratio (m^2/kg)
a is the orbit semi-major axis (m)
ρ is the atmospheric density (kg/m^3)

Then

$$PN2D = \left(\frac{\delta t}{2\pi/n}\right)\left(\frac{\Delta h}{\delta h}\right)$$

where δt is the simulation time step in seconds and δh is the object matrix altitude bin size in kilometers.

2.4.5 Probability of Satellite Becoming Non-Maneuverable

The probability of a maneuverable satellite transitioning to the non-maneuverable state (PM2N) is the probability of loss of maneuverability. This can occur either due to a failure mechanism or a small object collision. It is modeled based on the estimated satellite lifetime, satellite failure rate over lifetime, and probability of maneuverability being lost due to a small object collision

$$PM2N = \frac{SatellitFailureRate \times \delta t}{31{,}557{,}600 \times SateliteLifetime} + SmallCollisionFactor \times PN2F$$

where δt is the simulation step size in seconds and SatelliteLifetime is in years.

The small collision factor is set to 5.3 assuming that only 20% of the collisions with debris between 1 cm and 10 cm result in loss of maneuverability and noting that ESA estimates [13] that there are 900,000 debris objects in that range compared to 34,000 above 10 cm (0.2 x 900,000 / 34,000 = 5.3).

2.5 Object Life Process Models

The launch, decay, and fragmentation processes manage the life cycle of the objects.

2.5.1 Launch Process

The launch process maintains the LC(s) being evaluated at a fixed size for the duration of the analysis. The appropriate object flux matrix (SML, SMM, or SMS) is updated by maintaining a constant number of satellites in the object matrix cell corresponding to the orbit (altitude and inclination) of each LC at each timestep.

2.5.2 Decay Process

The decay process moves non-maneuverable objects to the next lower row of the object matrix. If an object in the h_1 row decays, it is assumed to have completed deorbit, and is removed from the object matrix. For maneuverable satellites, the decay process moves them to a 300-km circular disposal orbit as non-maneuverable satellites.

2.5.3 Fragmentation Process

When a collision occurs, the fragmentation process removes the objects involved from the associated object matrices, determines the numbers and characteristics of the fragments, and adds the new objects to the appropriate debris matrices. Fragments with perigee <200 km or mean altitude outside the 200 km to 2,000 km LEO range are dropped from the model.

The Fragmentation Process is modeled based on the MASTER-8 version of the EVOLVE 4.0 NASA Standard Breakup Model for spacecraft [15]. The number of fragments is determined from a power law distribution characterized by the object masses and the minimum and maximum object sizes. It is well known that the NASA model does not conserve mass, and many workarounds have been proposed. However, for this analysis, the important quantiles are the number of fragments, their diameter distribution, and their velocity distribution.

The number of fragments with size in the range from d_{MIN} (m) to d_{MAX} (m) is given by

$$N = 0.1(m_S + m_P)^{0.75}(d_{MIN}^{-1.71} - d_{MAX}^{-1.71})$$

Assuming that all collisions are fragmenting (specific kinetic energy of projectile, $\frac{m_P v_I^2}{2m_S}$, greater than 40 J/g) and truncating at a minimum fragment size to d_{MIN} and maximum fragment size to d_{MAX}, the cdf for fragment diameter is given by

$$cdf(d_F) = \frac{d_F^{-1.71} - d_{MAX}^{-1.71}}{d_{MIN}^{-1.71} - d_{MAX}^{-1.71}}$$

Area-to-mass ratio is characterized by a bi-normal distribution parametrized based on $\delta = log_{10}(d_F)$ for $\chi = log_{10}(A/M_F)$

$$\rho(\chi, \delta) = \alpha \frac{1}{\sigma_1\sqrt{2\pi}} e^{-(\chi-\mu_1)^2/(2\sigma_1)} + (1-\alpha)\frac{1}{\sigma_2\sqrt{2\pi}} e^{-(\chi-\mu_2)^2/(2\sigma_2)}$$

where the parameters α, μ_1, μ_2, σ_1, and σ_2 are functions of δ.

The fragment delta velocity (m/s) is related to the fragment A/M (m^2/kg) for fragmenting collisions by

$$cdf(v) = \frac{1}{2}\left(erf\left(\frac{v - 0.2\chi - 1.85}{0.4\sqrt{2}}\right) + 1\right)$$

The delta velocity is uniformly distributed over a sphere, added to the state vector for a randomly located object in the original orbit, and the resulting state vector converted to orbital elements to determine the delta altitude and inclination of each fragment relative to the original orbit.

The number of fragments and distributions for the fragment diameters, area-to-mass ratio, and delta altitude are shown in Fig. 3 for d_{MIN} = 0.1 m and d_{MAX} = 3 m.

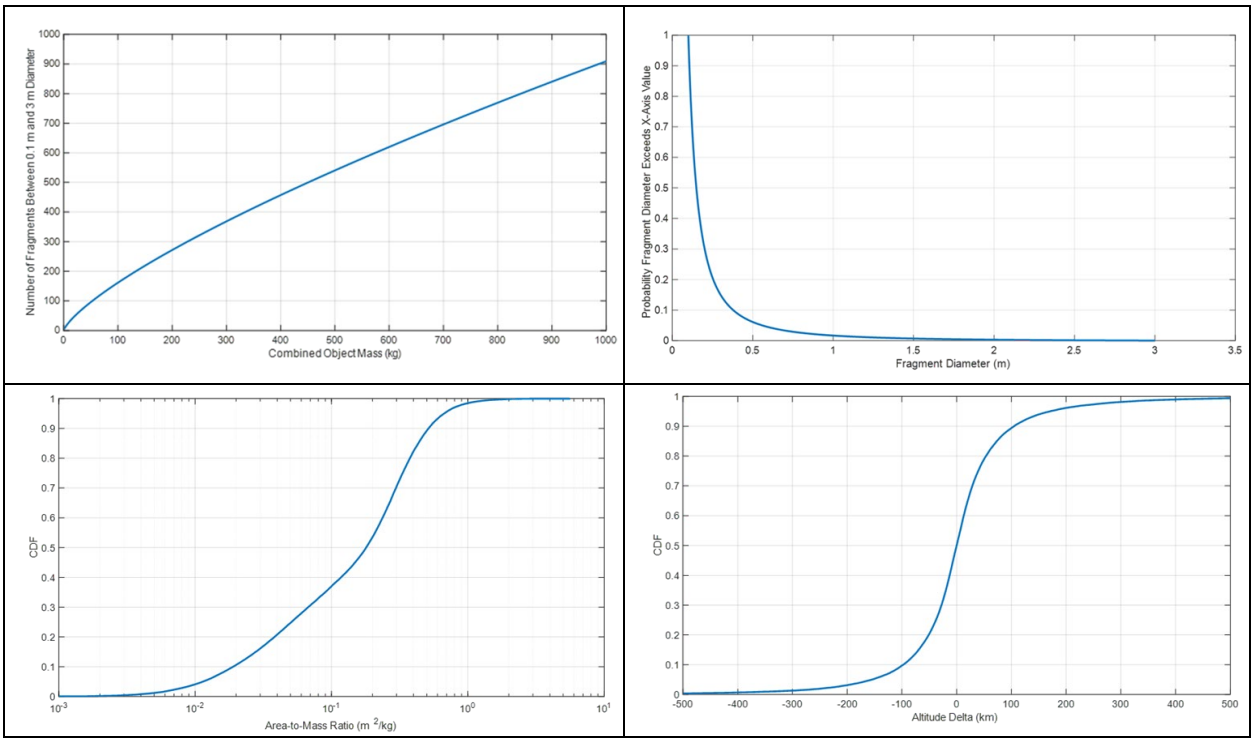

Fig. 3. Fragmentation Process Distributions

3. SIMULATIONS

Monte Carlo simulations are used to characterize the debris population sensitivity to LC orbits and satellite sizes over one hundred years, or until a Kessler Syndrome occurs. The simulation flow is shown in Fig. 4.

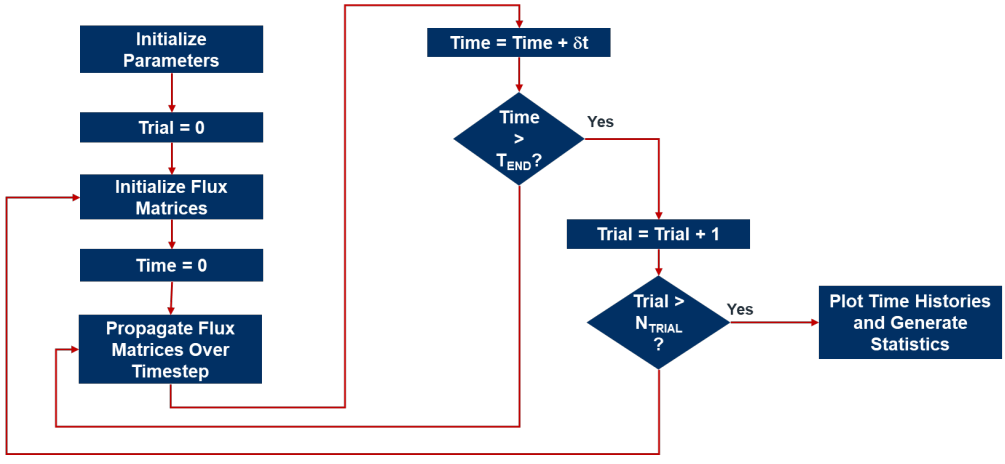

Fig. 4. Simulation Flow

Initially, 146 cases were run, a baseline case with the initial object matrices and no new satellite launches, and an additional 145 cases based on 29 configurations (combinations) of small (15 kg), medium (250 kg), and/or large (500 kg) satellites in the three orbits considered. Each configuration results in 5 cases with 10,000, 20,000, 30,000, 40,000, or 50,000 satellites maintained in each orbit. Depending on the case, from 10,000 to 150,000 satellites are maintained in orbit.

The simulation parameters are summarized in Tab. 2. The start year is used to determine the solar flux at each time step, which is used to compute the atmospheric density in Section 2.4.4. The 100-year duration was selected to focus on near-term (in a cosmic sense) events. The time step, altitude bin size, and inclination bin size are selected to provide reasonable simulation times. Reducing the first two by an order of magnitude did not significantly change the results. Reducing the inclination step size by an order of magnitude resulted in an observable increase in the time to Kessler Syndrome but did not change the relative times between cases. LC satellites typically range from 3 to 10 year predicted lifetimes; 5 years is selected as a representative value. The ODMSP [16] requires that LC satellites have a 90% probability of successful post mission disposal with a goal of 99%. The 5% failure rate (95% success rate) is chosen to be in the middle of this range. The small constellation factor is discussed in Section 2.4.5 and avoidance failure rate in Section 2.4.2. Sensitivity analysis was not preformed with respect to the last 4 parameters.

Tab. 2. Simulation Parameter Summary

Parameter	**Value**
Start Year	2021
Duration	100 years
Time Step (δt)	15 days
Altitude Bin (δh)	25 km
Inclination Bin (δi)	10°
Lifetime	5 years
Failure Rate	5%
Small Collision Factor	5.3
Avoidance Failure Rate	0.1%

The baseline case does not result in a Kessler Syndrome after 100 years. Tab. 3 shows the time to Kessler syndrome (years) for the remaining 145 cases. There are twenty-nine rows for the configurations and 5 columns for the number of satellites per orbit. The Satellite Size/Orbit columns indicate which orbits are populated for each configuration and with which size satellites: S – small (15 kg), M – medium (250 kg), or L – large (500 kg). For example, the Configuration 1 / 10K case is 10,000 small satellites in 450-km orbits, for that case a Kessler Syndrome did not occur within 100 years. Another example, the Configuration 22 / 30K case is 30,000 small satellites in 450-km orbits and 30,000 medium satellites in 600-km orbits, that case results in Kessler Syndrome in 23.4 years.

It is seen that the number of satellites, the satellite size, and the orbit altitude all matter. None of the cases consisting of only small (15-kg) satellites experiences a Kessler Syndrome within 100 years. This includes the 150,000-satellite case with 50,000 satellites in each orbit. The cases with at least 30,000 medium (250-kg) satellites in the 600-km or 1,200-km orbits experience a Kessler Syndrome within 25 years. The cases with at least 10,000 large (500-kg) satellites in the 600-km or 1,200-km orbits experience a Kessler Syndrome within 12.5 years.

Configurations 28 and 29 are interesting. In Configuration 28, small satellites (15-kg) are maintained in the 450-km orbit and large satellites (500-kg) in the 1,2000-km orbit. In Configuration 29, the sizes are reversed, large in 450-km and small in 1,200-km. In both configurations, medium satellites are maintained in the 600-km orbit. The time to Kessler Syndrome for of the numbers of satellites per orbit is from 3 to over 10 times longer for the Configuration

29 cases. All these cases have the same number of satellites and the same total mass in orbit. The only difference is the switch of which orbits the small and large satellites occupy. Clearly, the larger satellites in lower orbit are safer than the larger satellites in higher orbit.

Four cases are explored in more detail. The baseline case in Section 3.1, the 150,000 small satellite case in Section 3.2, the 30,000 medium satellite 600-km orbit case in Section 3.3, and the 10,000 large satellite 1,200-km orbit case in Section 3.4.

Tab. 3. Time to Kessler Syndrome (Years)

	Satellite Size/Orbit			Satellites Per Orbit				
Configuration	450 km	600 km	1200 km	10K	20K	30K	40K	50K
1	S			>100	>100	>100	>100	>100
2	M			>100	>100	>100	>100	>100
3	L			>100	>100	>100	>100	>100
4		S		>100	>100	>100	>100	>100
5		M		>100	>100	22.1	13.5	11.2
6		L		11.3	5.8	4.2	3.8	3.0
7			S	>100	>100	>100	>100	>100
8			M	29.9	18.0	14.5	12.0	10.4
9			L	10.0	6.3	5.0	4.1	3.3
10	S	S		>100	>100	>100	>100	>100
11	M	M		>100	>100	23.7	13.0	11.9
12	L	L		12.5	6.4	4.3	3.6	3.1
13	S		S	>100	>100	>100	>100	>100
14	M		M	29.9	18.8	14.7	11.6	10.1
15	L		L	9.8	6.9	4.8	3.9	3.5
16		S	S	>100	>100	>100	>100	>100
17		M	M	29.7	18.4	14.6	11.7	10.2
18		L	L	9.7	6.0	4.5	3.7	3.0
19	S	S	S	>100	>100	>100	>100	>100
20	M	M	M	29.8	18.8	14.2	11.9	10.1
21	L	L	L	10.2	6.2	4.4	3.7	3.0
22	S	M		>100	>100	23.4	13.6	11.7
23	L	M		>100	>100	22.0	13.1	11.1
24	S		L	9.8	6.9	5.1	4.0	3.4
25	L		S	>100	>100	>100	>100	>100
26		M	S	>100	>100	22.5	13.5	11.2
27		M	L	8.8	6.7	4.7	3.7	3.5
28	S	M	L	10.0	6.6	5.1	3.9	3.5
29	L	M	S	>100	>100	20.5	13.5	11.3

3.1 Baseline Case

The time evolution of the baseline case is shown in Fig. 5. The maneuverable (active) satellites (solid lines) completely decay due to the 5-year lifetime model and post mission disposal of maneuverable satellites. The number of rocket bodies (dash-dot-dash line) decreases due to drag and collisions. The number of non-maneuverable (passive) satellites (dashed lines) deceases initially due to decay at the lower altitudes and then stabilizes. The debris (dotted lines) are observed to grow exponentially with an approximately 6-year time constant until the active satellites decay, and then at a much slower rate (approximately 100-year time constant).

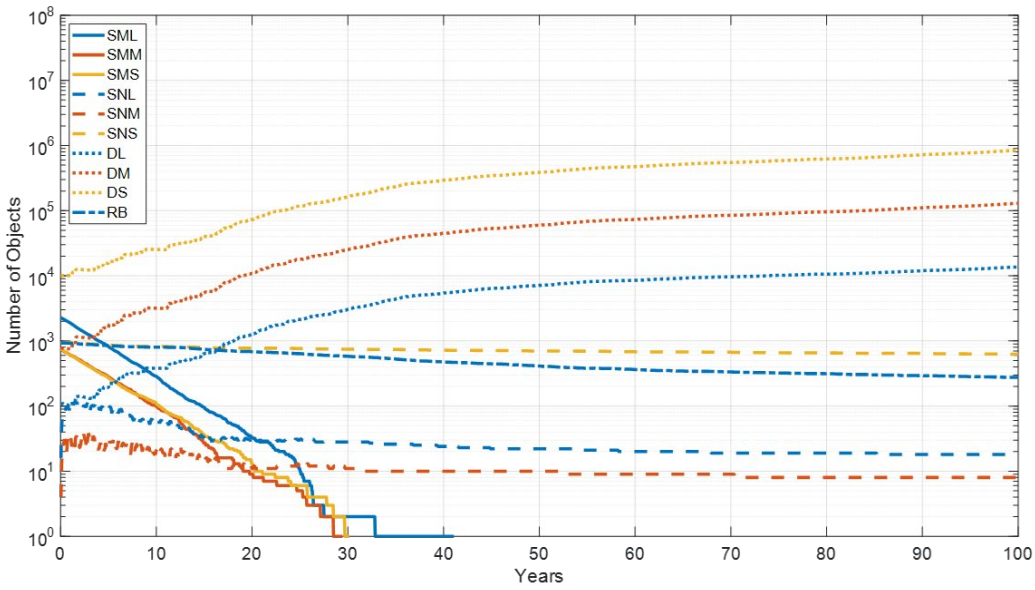

Fig. 5. Baseline Case Evolution by Class

Fig. 6 compares the object fluxes at the start of simulation and at the end, 100 years later. After 100 years, debris growth has increased the number of objects in the orbits that had the higher object concentrations.

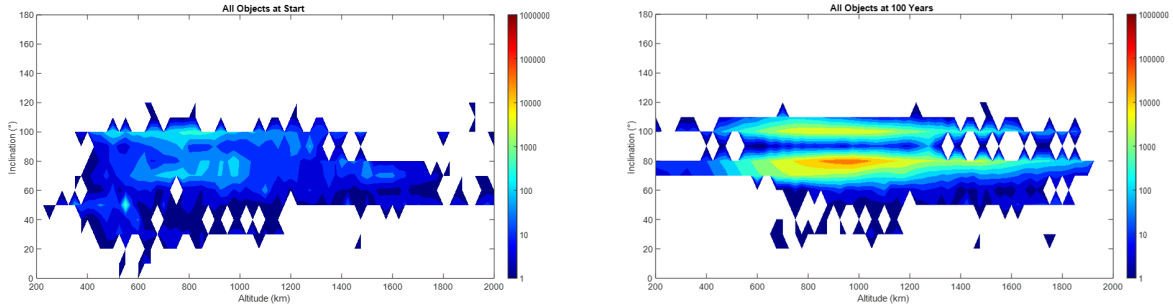

Fig. 6. Baseline Case Comparison from Start to 100 Years

The evolution of objects by altitude in the baseline case is shown in Fig. 7. An interesting feature is the clear indication of the solar cycle in the decay below 400 km. It is also interesting to note the spread of objects into higher orbits over time. As there are no new launches, the only mechanism for this in the model are fragmentation events.

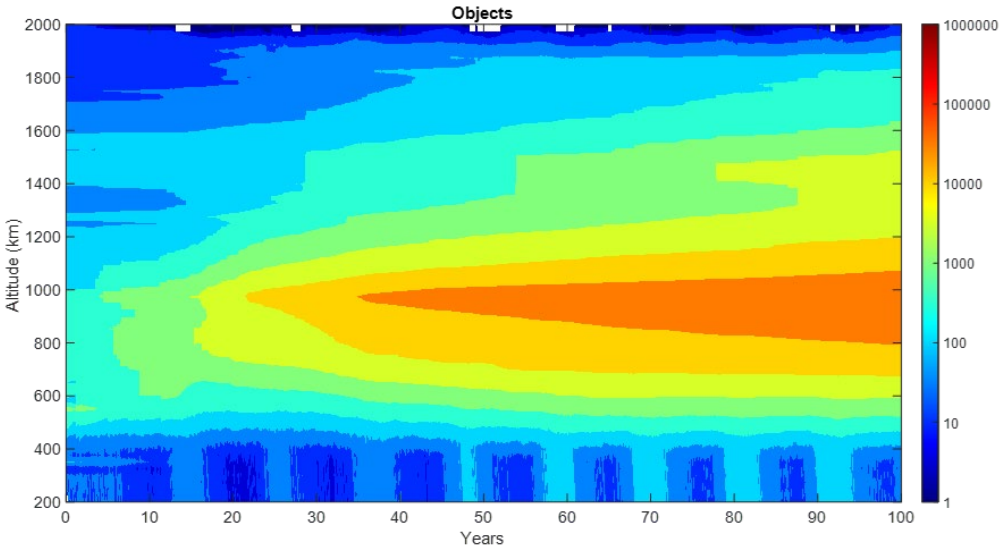

Fig. 7. Baseline Case Evolution by Altitude

3.2 150,000 Small Satellites Case (Configuration 19 / 50K)

In this case the LCs consist of 50,000 small satellites in the 450-km orbits, 50,000 small satellites in the 600-km orbits, and 50,000 small satellites in the 1,200-km orbits, for a total of 150,000 satellites. After 100 years, there is little difference in object distribution by orbit compared to the baseline (no new launches) case, as shown in Fig. 8. The additional objects around 1,200 km are from the operational satellites at that orbit, the debris spread around that orbit, and the non-maneuverable satellites decaying from that orbit.

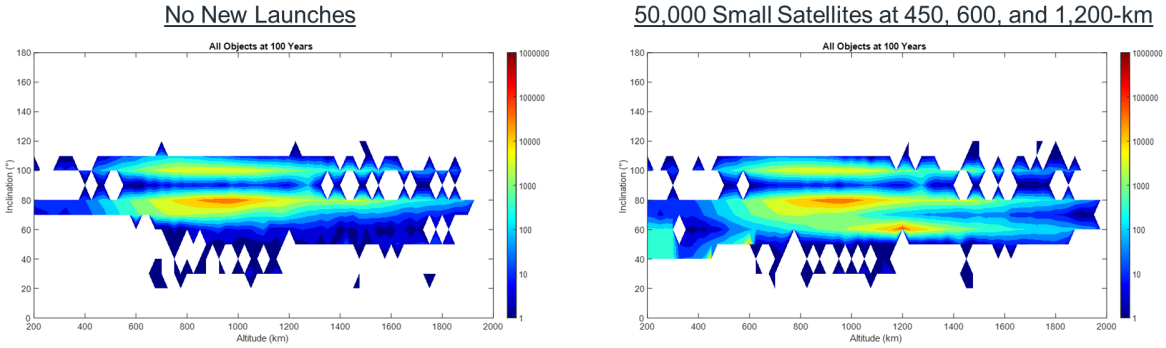

Fig. 8. Comparison of Baseline and 150K Small Satellite Cases at 100 Years

3.3 30,000 Medium Satellite at 600-km Orbit Case (Configuration 5 / 30K)

In this case the LC consists of 30,000 medium satellites in the 600-km orbits. The result is a Kessler Syndrome in slightly more than 22 years, consuming the satellites in that orbit and creating millions of debris objects. The evolution of the object classes in shown in Fig. 9. The SMM curve jumps to 30,000 at time zero and continues at that level until just before the Kessler Syndrome when the satellites are consumed by the debris. Fragmentation of LC satellites that lose maneuverability due to failures or small object collisions cause the increase in the SNM curve. Fragments from these non-maneuverable satellites as they experience collisions result in the increases of the DL, DM, and DS curves. The approximately 11,000 lethal debris objects at time zero grows to over 33 million at the start of Kessler Syndrome.

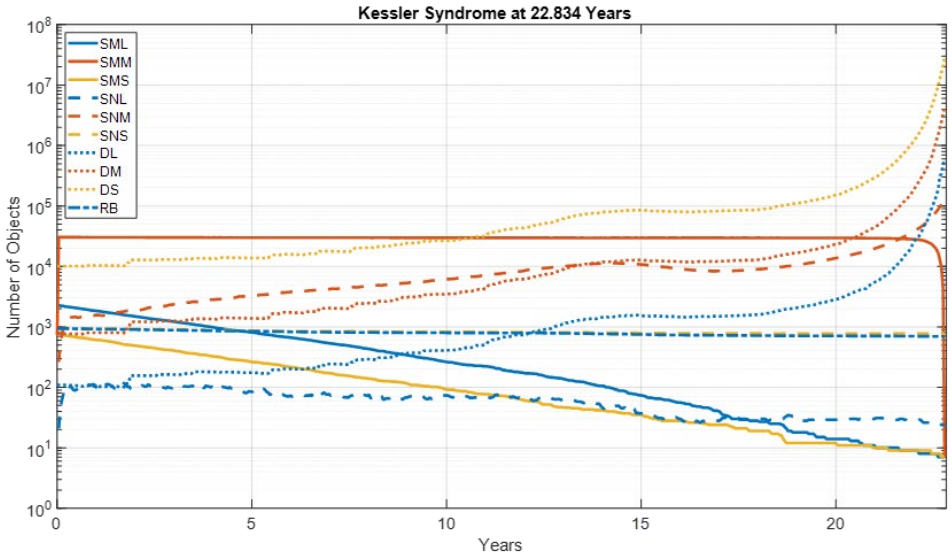

Fig. 9. 30,000 Medium Satellites at 600-km Initiate Kessler Syndrome in 22 Years

The debris evolution by altitude is shown in Fig. 10. The spike in debris around 600-km leading to the Kessler Syndrome is apparent.

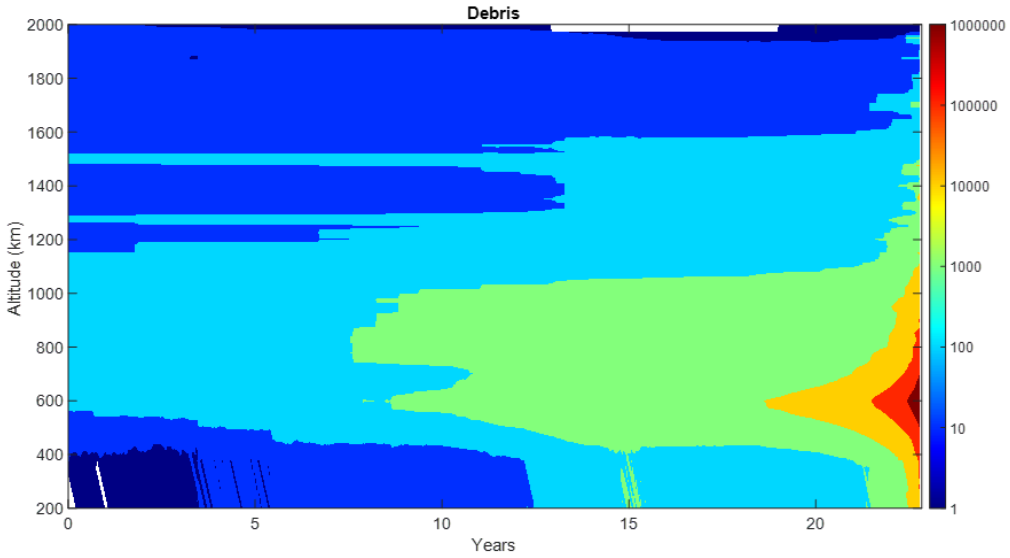

Fig. 10. 30,000 Medium Satellites at 600-km Case – Debris Evolution by Altitude

An interesting question raised by these results – when is the tipping point? Additional simulations were run to address this question for the 30,000 medium satellites in the 600-km orbit case. The previous results showed a Kessler Syndrome occurring in 22 years. Stopping launches after year 15 was found to reliably avoid a Kessler Syndrome within the 100-year simulation time.

Fig. 11 compares the object evolution for the continuous launch and the launch stop after 15 years cases. Note that the time scales are different. The continuous launch case plot ends at the time of Kessler Syndrome while the stop after 15 years case plot continues for 100 years.

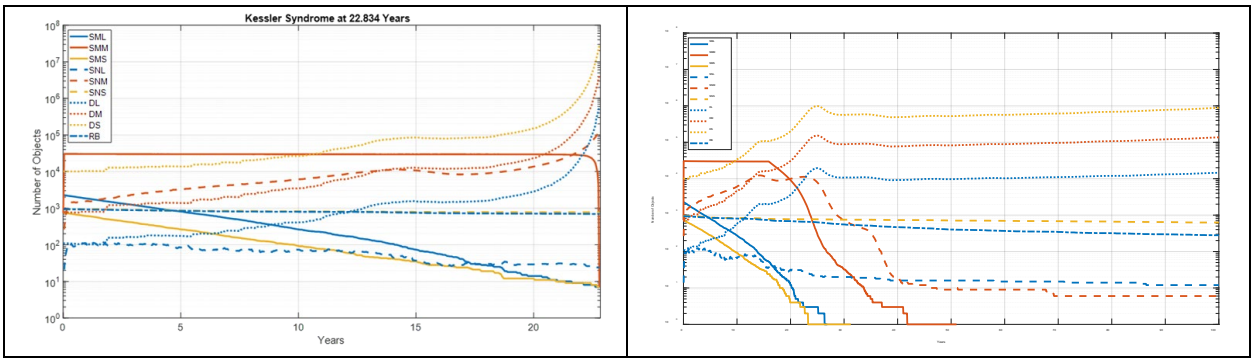

Fig. 11. Comparison of Object Evolution – Continuous Launch (left) vs. Launch Stop After 15 Years (right)

As shown in Fig. 12 and Fig. 13, stopping launches after 20 years delays the Kessler Syndrome by 4 years but does not prevent it – the tipping point has been reached.

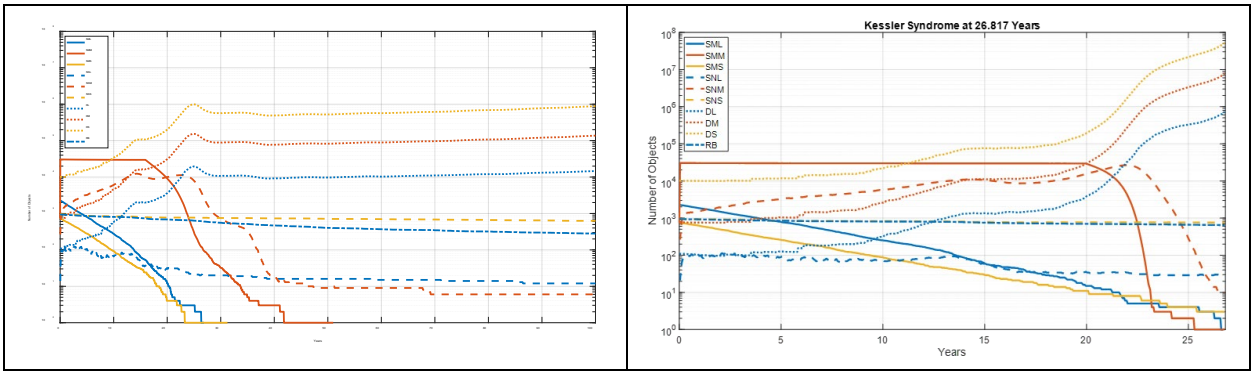

Fig. 12. Comparison of Object Evolution – Stop After 15 Years (left) vs. Stop After 20 Years (right)

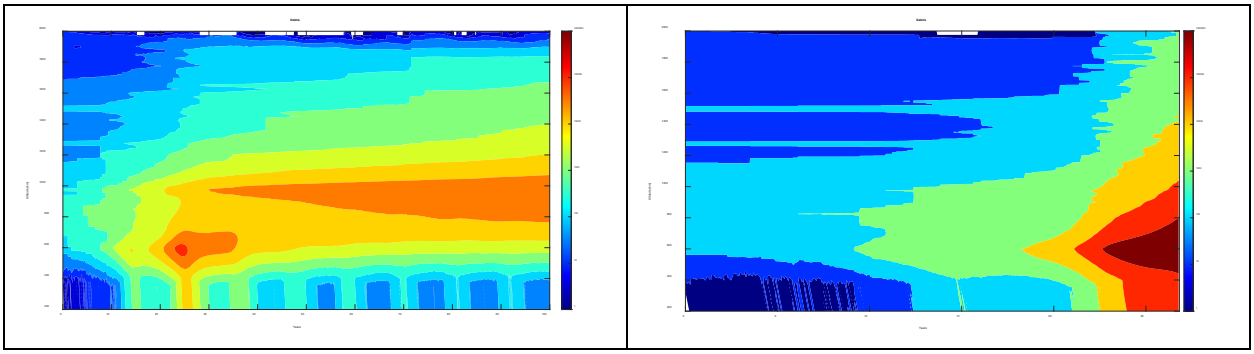

Fig. 13. Comparison of Debris Evolution by Altitude – Stop After 15 Years (left) vs. Stop After 20 Years (right)

3.4 10,000 Large Satellites in 1,200-km Orbit Case (Configuration 9 / 10K)

In this case the LC consists of 10,000 satellites in the 1,200-km orbit. The result is a Kessler Syndrome in 10 years. The object evolution is shown in Fig. 14. The SML curve jumps to 10,000 at time zero and continues at that level until just before the Kessler Syndrome when the satellites are consumed by the debris. The tail of the curve are the remaining large satellites from the baseline case at orbit altitudes away from the debris spike. Fragmentation of LC satellites that lose maneuverability due to failures or small object collisions cause the increase in the SNL curve.

Fragments from these non-maneuverable satellites as they experience collisions result in the increases of the DL, DM, and DS curves.

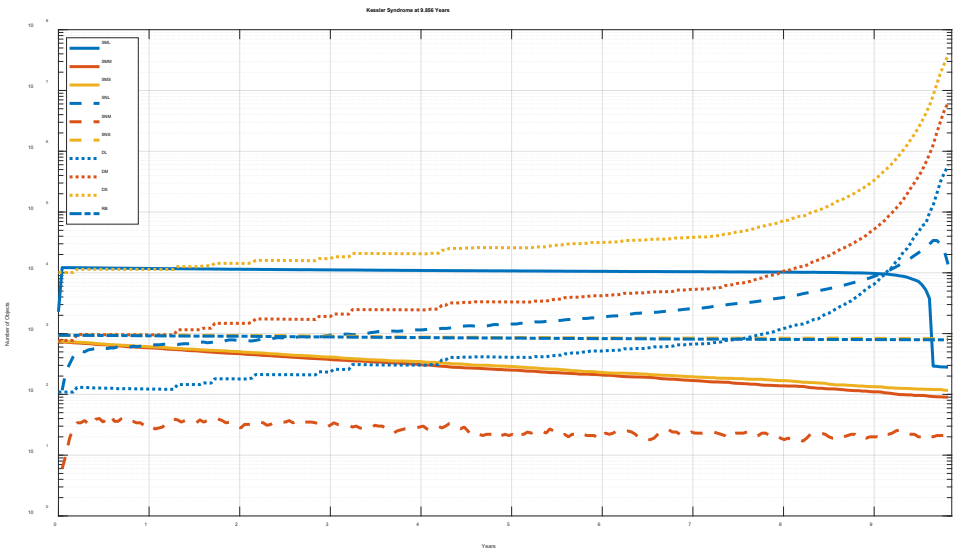

Fig. 14. 10,000 Large Satellites at 1,200-km Initiate Kessler Syndrome in 10 Years

These results lead to the question of how many large satellites can be supported in the 1,200-km orbit. Additional simulations were run to address this question. The results are summarized in Fig. 15. With a constellation of 200 large satellites maintained at 1,200-km, Kessler Syndrome did not occur within 100 years. With 500 satellites, Kessler Syndrome occurred in 72 years, and with 1,000 satellites in 48 years.

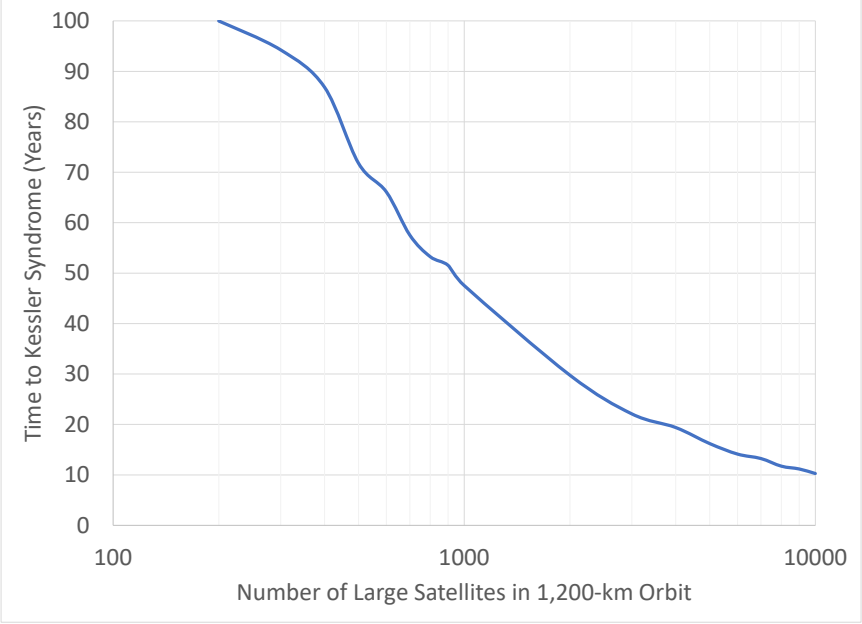

Fig. 15. Time to Kessler Syndrome vs. Number of Large Satellites in 1,200-km Orbit

4. CONCLUSIONS

The simulation results show that: 1) LCs of small satellites (<25 kg) are significantly safer than LCs of medium (25 to 300 kg) or large (>300 kg) satellites, and 2) if LCs of medium or large satellites are deployed, they are safer at lower orbits, such as 450-km rather than at 600-km or 1,200 km orbits. LC operators can reduce the risk of a Kessler Syndrome by deploying small (<25-kg) satellites, or if deploying medium or large satellites doing so at low orbits (such as 450-km) rather than at higher orbits (such as 600-km or 1,200-km).

The results also demonstrate the concepts of orbital capacity (the number and type of satellites that can be sustainably deployed in each orbit without risking a Kessler Syndrome) and tipping points (point in time at which it is no longer possible to avoid a Kessler Syndrome by ceasing launches). Section 3.3 showed a case where a Kessler Syndrome can be reliably avoided by ceasing launches after a certain year but that if launches are continued for a few more years, it is too late. Section 3.4 showed a case where an orbit has a capacity, if a threshold number of a certain size satellite are maintained in that orbit, a Kessler Syndrome will not occur, but if the threshold is exceeded, it will occur. Future work will refine the simulation models to improve fidelity and further investigate orbital capacity and tipping points.

5. REFERENCES

[1] B. Shivali, 'A disaster waiting to happen': Space junk left behind by humans has formed the equivalent of a 'drifting island of plastic' in low-Earth orbit, expert warns. *Daily Mail*, January 12, 2021, https://www.dailymail.co.uk/sciencetech/article-9138879/Orbiting-space-debris-new-drifting-island-plastic.html

[2] G. Long, *The Impacts of Large Constellations of Satellites*, JASON – The MITRE Corporation, JSR-20-2H, November 2020, (Updated: January 21, 2021).

[3] Space-Track Satellite Catalog, https://www.space-track.org/#catalog (retrieved 18 August 2021).

[4] M. A. Sturza and G. Saura Carretero, Mega-Constellations – A Holistic Approach to Debris Aspects, *Proc. 8th European Conference on Space Debris*, May 2021.

[5] D. J. Kessler and B. G. Cour-Palais, Collision Frequency of Artificial Satellites: The Creation of a Debris Belt. *Journal of Geophysical Research*. 83 (A6): 2637–2646, 1978.

[6] D. Lambach, and L. Wesel, Tackling the Space Debris Problem: A Global Commons Perspective, *Proc. 8th European Conference on Space Debris*, May 2021.

[7] M. Undseth, C. Jolly, M. Olivari, The Economics of Space Debris in Perspective, *Proc. 8th European Conference on Space Debris*, May 2021.

[8] Space Sustainability – The Economics of Space Debris in Perspective, *OECD Science, Technology and Industry Policy Papers*, April 2020 No. 87.

[9] A.C. Boley and M. Byers, Satellite mega-constellations create risks in Low Earth Orbit, the atmosphere and on Earth, *Sci Rep* 11, 10642. 2021.

[10] S. Kawamoto, N. Nagaoka, Y. Kitagawa, and T. Hanada, Evaluation of Impacts of Large Constellations Using a Debris Evolutionary Model for Considering Environment Capacity, *Proc. 8th European Conference on Space Debris*, May 2021.

[11] H. G. Lewis and N. Marsh, Deep Time Analysis of Space Debris and Space Sustainability, *Proc. 8th European Conference on Space Debris*, May 2021.

[12] M. Rathnasabapathy, et. al., Space Sustainability Rating: Designing a Composite Indicator to Incentivize Satellite Operators to Pursue Long-Term Sustainability of the Space Environment, *71st International Astronautical Congress (IAC) – The CyberSpace Edition*, 12-14 October 2020.

[13] ESA Space Environment Statistics, https://sdup.esoc.esa.int/discosweb/statistics/ (retrieved 25 August 2021).

[14] D. A. Vallado, *Fundamentals of Astrodynamics and Applications*, Fourth Edition, Microcosm Press, 2013.

[15] A. Horstmann, S Hesselbach, C. Wiedemann, S. Flegel, and M. Oswald, *Final Report – Enhancement of S/C Fragmentation and Environment Evolution Models*, DD-0045, Institute of Space Systems, Technische Universität Braunschweig, 2020.

[16] U.S. Government, *Orbital Debris Mitigation Standard Practices*, November 2019 Update, https://orbitaldebris.jsc.nasa.gov/library/usg_orbital_debris_mitigation_standard_practices_november_2019.pdf